

UNCLASSIFIED

Copy

6

RM A55F23

NACA RM A55F23



RESEARCH MEMORANDUM

PRELIMINARY EXPERIMENTAL INVESTIGATION OF A VARIABLE-AREA,
VARIABLE-INTERNAL-CONTRACTION AIR INLET AT MACH
NUMBERS BETWEEN 1.42 AND 2.44

By Richard Scherrer and Forrest E. Gowen

Ames Aeronautical Laboratory
Moffett Field, Calif.

CLASSIFICATION CHANGED

To

UNCLASSIFIED

By authority of *NASA TPA 9* *Effective* Date *9-1-59*

71B 11-23-59

CLASSIFIED DOCUMENT

This material contains information affecting the National Defense of the United States within the meaning of the espionage laws, Title 18, U.S.C., Sec. 793 and 794, the transmission or revelation of which in any manner to an unauthorized person is prohibited by law.

NATIONAL ADVISORY COMMITTEE FOR AERONAUTICS

WASHINGTON

September 7, 1955

11-23-59

SEP 11 1955

AMES AERONAUTICAL LABORATORY
Moffett Field, California

UNCLASSIFIED



3 1176 01434 8636

NATIONAL ADVISORY COMMITTEE FOR AERONAUTICS

RESEARCH MEMORANDUM

PRELIMINARY EXPERIMENTAL INVESTIGATION OF A VARIABLE-AREA,

VARIABLE-INTERNAL-CONTRACTION AIR INLET AT MACH

NUMBERS BETWEEN 1.42 AND 2.44

By Richard Scherrer and Forrest E. Gowen

SUMMARY

A preliminary investigation of a variable-area, variable-internal-contraction air inlet was conducted at Mach numbers from 1.42 to 2.44. All tests were performed with the model at zero angle of attack. The Reynolds numbers of the tests based on inlet width ranged from 0.4×10^6 to 1.6×10^6 . The total pressure recovery after supersonic compression, the total pressure recovery at the exit of the subsonic diffuser and the pressure distribution along the diffuser walls were measured. The inlet was tested with both rectangular and modified internal cross sections. The maximum total pressure recovery obtained for the design range of Mach numbers was sufficiently near that obtained with other variable inlets to warrant further investigation.

INTRODUCTION

It is necessary for some aircraft to operate efficiently at a variety of Mach numbers and over a wide range of altitudes. These aircraft, to attain the maximum net propulsive force, require some form of variable inlet. A number of variable inlets have been proposed (refs. 1 through 10) and sufficient experimental data are available to allow the designer to make detailed evaluations of most of these inlets. Little data are available, however, for inlets having both the inlet area and the contraction ratio independently variable. Since such inlets in theory have as good or better pressure recovery and less spillage drag than other variable inlets, experimental investigations are warranted.


UNCLASSIFIED

The purpose of the present investigation was to determine the pressure recovery of one variable-internal-contraction inlet for a variety of entrance areas and contraction ratios. These data and the fact that the mass-flow ratio can always be maintained at unity for practical operational conditions are sufficient for evaluation of the net propulsive force of an engine installation employing such an inlet. The inlet selected for test had rectangular cross sections, variable entrance area, variable internal contraction, and sharp lips.

SYMBOLS

A	inlet cross-sectional area, sq in.
L	inlet length from leading edge of side plate to rake station, in.
m	inlet mass-flow rate, slugs/sec
M	Mach number
p	static pressure, lb/sq in.
P _t	total pressure, lb/sq in.
q	dynamic pressure, lb/sq in.
R	Reynolds number based on duct width
x	longitudinal distance from leading edge of side plate, in.
y	distance from fixed plate to movable flap (fig. 1), in.
y _{1e}	equivalent throat height, throat area/throat width, in.
δ	diffuser flap angle, deg
θ _c	equivalent conical subsonic diffuser angle, deg

Subscripts

o	free-stream conditions at entrance to inlet
1	inlet throat station
2	diffuser exit station
av	average

d subsonic diffuser flap
f front flap
isen conditions for isentropic flow

APPARATUS AND TESTS

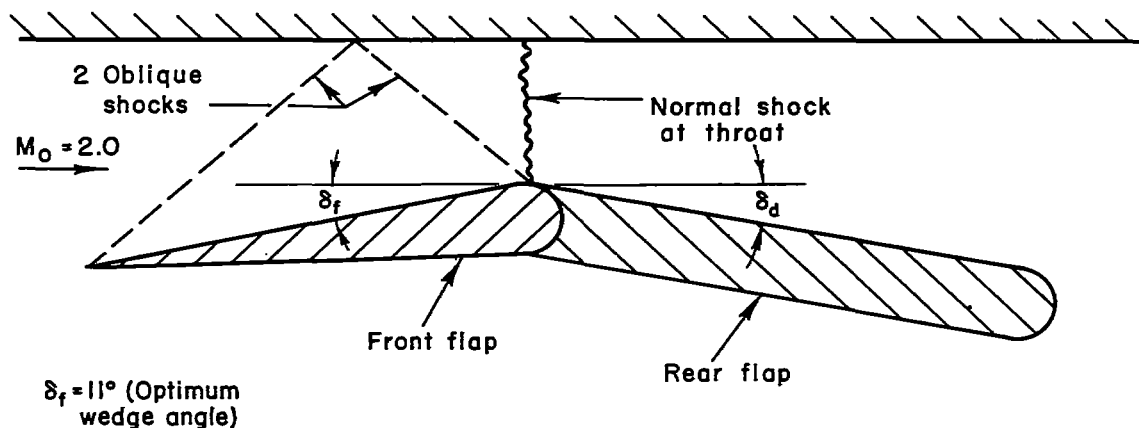
Wind Tunnels

The first tests of this investigation were performed in the Ames 8-by 8-inch supersonic wind tunnel. This tunnel is a continuous-operation, atmospheric-discharge wind tunnel equipped with an asymmetric sliding-block nozzle for varying the test-section Mach number. Tests were performed at a Mach number of 1.90 and a Reynolds number based on inlet width of 1.60×10^6 . A detailed description of the tunnel and its auxiliary equipment is presented in reference 11.

Since tests at Mach numbers less than 1.90 could not be run in the 8-by 8-inch wind tunnel due to tunnel blockage by the model and its supports, a second series of tests was run in the 1- by 3-foot supersonic wind tunnel No. 1. This wind tunnel is a continuous-operation, variable-pressure wind tunnel equipped with flexible top and bottom plates for varying the test section Mach number. Tests at free-stream Mach numbers of 1.42, 1.75, and 2.44 were made at a Reynolds number, based on inlet width, of about 0.82×10^6 . Tests at a Mach number of 1.99 were made at Reynolds numbers of 0.40, 0.84, and 1.10×10^6 .

Model

The model was designed to allow operation as a normal-shock inlet, and at the design Mach number of 2.0, as a three-shock inlet. The two-dimensional, three-shock configuration for optimum pressure recovery at the design Mach number was selected and is shown in the following sketch:



A great number of shock configurations other than that shown in the sketch could be obtained both at the design and at off-design Mach numbers, because the entrance and throat areas could be controlled independently. This permits the experimental optimum shock configuration to be determined at each Mach number. At Mach numbers below about 1.5 the inlet was assumed to operate as a variable-entrance-area, normal-shock inlet.

The flow requirements of an existing turbojet engine were used to determine the ranges of entrance to throat area variations that were employed in the mechanical design of the model. These area ratios and the shock configuration for optimum pressure recovery at the design point (which specifies the angle of the front flap) determine the length of the front flap. The length of the rear flap was selected so that the maximum divergence angle at the design condition was about $6-1/2^\circ$. This angle was considered to be a reasonable compromise between the requirements of minimum flap length (to minimize weight) and of maximum subsonic diffuser efficiency.

A sketch of the model and instrumentation is shown in figure 1. Flap control mechanisms were so arranged that the position of either flap could be changed during a test. Throat heights from 1.0 to 1.58 inches and lip heights from 1.0 to 2.1 inches were provided. The variations of front flap angle and entrance area with throat height for various contraction ratios are shown in figure 2.

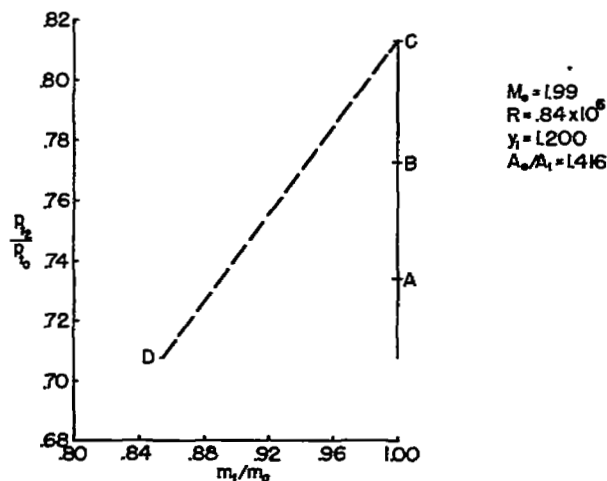
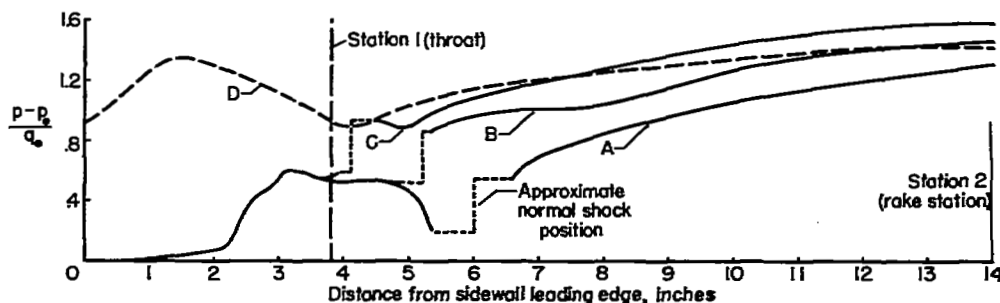
Near the end of the test program two modifications consisting of inserts as shown in figure 3 were made to the model. The purpose of these inserts was to cause a more uniform rate of pressure rise. The fillets, in addition, reduced the wetted area slightly for a given contraction ratio. The curve of longitudinal distribution of cross-sectional area with the wedge insert installed was composed of linear segments, as were the distributions for the unmodified model. (These distributions are directly obtainable from the model dimensions, figs. 1 and 3.) The addition of fillets caused only a slight deviation from linearity. The changes in the subsonic diffuser which occurred with varying throat height for both unmodified and modified models are shown in figure 4.

Instrumentation

The model was instrumented as shown in figure 1 to give static-pressure distributions along the top plate and on one side plate. The 16 uniformly spaced total-pressure tubes located at the rake station were used to obtain the total-pressure distribution and were averaged to obtain the effective pressure recovery. Mass-flow rates through the model were measured with an ASME orifice meter located as shown in figure 1 as well as from calculations of the entering mass flow based on free-stream conditions and entrance area. In general, the two methods agreed within 1-1/2 percent. Drag data were not obtained with the present model.

Test Procedure

The test procedure for a given wind-tunnel setting (i.e., Mach number and Reynolds number) and a given throat setting of the model involved two separate operations, namely, the determination of the maximum contraction ratio for supersonic inlet flow and the determination of the maximum pressure recovery for each throat height. With a given throat setting and minimum back pressure (normal shock downstream of the throat) the front flap was moved so that the entrance opened slowly to a point where the shock would pop out if the flap were opened further. The resulting entrance-to-throat-area ratio was denoted as the maximum contraction ratio for that particular set of test conditions. For this flap setting the back pressure was then increased by closing the throttle valve slowly, causing the normal shock to move upstream toward the throat. Static-pressure distributions and total-pressure recoveries were recorded for several positions of the normal shock. Typical static-pressure distributions for different shock positions are shown in the sketch below along with the corresponding pressure recoveries. Included in the sketch is one static-pressure distribution for subcritical operation of the inlet after a small increase in back pressure caused the normal shock to jump from the throat position (distribution "C") to a position just ahead of the inlet face (distribution "D").



The highest pressure recovery at which the inlet would run continuously without the normal shock moving out in front of the entrance was recorded as the maximum pressure recovery. It should be noted that for a given throat height, the maximum pressure recovery was not always obtained at the maximum contraction ratio.

Certain of the tests in the 1- by 3-foot supersonic wind tunnel No. 1 at the highest Reynolds numbers were restricted in the inlet-area variation available due to the limited pumping capacity of the wind-tunnel equipment. As a result, the largest throat openings could not be run at a Mach number of 2.44 or at the highest Reynolds number at a Mach number of 1.99.

RESULTS AND DISCUSSION

Pressure-Recovery Characteristics

Pressure recovery is usually presented as a function of mass-flow ratio. In the present investigation, however, the mass-flow ratio was always unity, so, for convenience, the pressure-recovery data in this report have been plotted against the dimensional parameter, throat height. In addition, the contraction ratio, A_0/A_1 , for each data point is shown. These plots, with those of figure 2, allow replotting of the data in several additional forms if desired.

The maximum total-pressure recoveries obtained with the unmodified inlet are presented in figure 5, and those for the inlet with the wedge or fillet inserts are shown in figure 6.¹ The results show that at all Mach numbers the maximum total-pressure ratio occurred at the greatest throat height available and indicated that the optimum throat height for best pressure recovery could not be attained because of mechanical limitations. For small throat heights at a Mach number of 1.90 (i.e., y_1 of 1.0 in. and 1.1 in. in fig. 5) the maximum pressure recovery was not obtained at the maximum contraction ratio, so both the maximum total-pressure ratio and the total-pressure ratio at maximum contraction ratio are included for comparison. Since the pressure recovered by supersonic compression is proportional to the contraction ratio, these results for small throat heights lead to the conclusion that the loss in pressure recovery due to viscous effects (e.g., shock-wave-boundary-layer interaction and separation) absorbed the gain in pressure recovery which resulted from the increased contraction ratio.

For the range of throat heights available with the present model, the maximum contraction ratio at each Mach number was essentially independent of throat height (figs. 5 and 6) except for a Mach number of 2.44, and for this Mach number the variation of maximum contraction ratio was not large.

¹For the model with fillet inserts the throat section is not rectangular and the effective throat height is considered to be the throat area divided by the throat width.

In figure 7, the maximum contraction ratios obtained from figures 5 and 6 with both the unmodified and the modified models at each Mach number are shown as a function of Mach number. Included in figure 7 are the line for maximum contraction for isentropic flow and the line for maximum contraction for starting the flow (corresponding to an initial normal-shock loss) in a fixed-contraction supersonic inlet (ref. 12). Comparison of the contraction ratios for the modified and unmodified inlets indicates that both the modifications resulted in improved pressure recovery at the throat (i.e., increased contraction). This increased pressure recovery and contraction is believed to be due to the more uniform rate of pressure rise, as can be seen by comparison of the curves of figures 8 and 9. However, an increase in pressure recovery at the throat did not always result in an increase in pressure recovery at the exit rake station. (See figs. 6(a) and (b).)

In order to obtain more accurate data on both the pressure recovered by supersonic compression p_{t1} and the duct losses between the throat and rake stations, a total-pressure survey was made near the throat with a single pitot tube at a test Mach number of 1.90. This pitot tube was located in the vertical center plane about 1/4 inch downstream of the model throat. Results of this survey corrected for normal-shock losses are shown in figure 10(a) along with the theoretical pressure recovery calculated from the pressure losses through the two oblique shocks ahead of the survey probe by use of the charts of reference 13. The center line distribution of total-pressure recovery at the rake station is shown in figure 10(b). Comparison of the distributions at the throat and rake stations indicates that the total-pressure losses between the free-stream and the throat station were about equal to those through the normal shock and in the subsonic diffuser.

The effect of Reynolds number on the performance of the inlet was investigated at a Mach number of 1.99. Results of these tests are presented in figure 11. The range of available Reynolds numbers was rather restricted and the throat heights for which data could be taken at the largest Reynolds numbers were limited by the capacity of the tunnel pumping equipment. An attempt was made to simulate higher Reynolds number test conditions by use of fine wires to cause transition to turbulent flow in the boundary layer. The results do not indicate an improvement in pressure recovery and it was concluded that the thickening of the boundary layer due to the transition wires had probably masked any favorable effect due to early transition. The results obtained without the trip wire indicate that there is a favorable effect on pressure recovery of increasing Reynolds number, but that additional tests are needed for a wide range of Reynolds numbers to establish trends more clearly.

The effect of typical inlet-operation conditions on the flow uniformity at the exit rake is illustrated in figure 12. Figures 12(a) and (b) show the comparison of normal-shock and internal-shock operation at Mach number 1.42. Although the region of highest pressure recovery is greater

for internal-shock operation, the average total-pressure recovery was less than for normal-shock operation (fig. 5). As would be expected from the data presented in figures 6, 8, and 9 for a Mach number of 1.99, a more uniform distribution of pressure ratio was obtained with the fillet and wedge inserts (figs. 12(g) and (h)) than with the unmodified inlet (fig. 12(e)).

The results of the present investigation indicate several design trends for variable-area, variable-internal-contraction inlets. As in all inlets, a major factor that limits pressure recovery is boundary-layer separation. The adverse effects of what appears to be separation have been shown to be reduced by increasing throat height which, with the present inlet, was accompanied by a reduction in the divergence angle of the subsonic diffuser. It appears probable that a more gradual change in slope of the variable wall near the throat would be advantageous. The effect of fillets was such as to indicate the desirability of nearly circular cross sections; thus, rapid, but fair, transitions from rectangular to circular sections are indicated. To be consistent with this trend, the duct cross section at the lip leading edge should have some corner radii at the fixed wall rather than square internal corners.

Comparison With Other Inlets

A comparison of the total-pressure recovery p_{t_2}/p_{t_0} obtained in the present investigation with the pressure recovery obtained with other variable-geometry inlets is made in figure 13. In this figure the curves for theoretical normal-shock recovery and theoretical optimum three-shock recovery, p_{t_1}/p_{t_0} , from reference 14 are included for comparison. Figure 13 is not presented to indicate relative over-all performance of variable inlets, for both pressure recovery and drag data are required for exact net propulsive-force evaluations for given operating conditions, and further research is necessary to provide data for such evaluations.

CONCLUDING REMARKS

The results of this preliminary investigation have indicated that the variable-area, variable-internal-contraction-inlet pressure recovery (e.g., total-pressure ratio of 0.89 at a Mach number of 1.90) is near that obtained with other variable-geometry inlets, even though the optimum geometry for maximum pressure recovery could not be obtained with the present model because of mechanical limitations. The net propulsive force was not evaluated because no drag measurements were made. However, since inlets of this type have neither spillage drag nor unsteadiness problems, and since the potential improvement appears large, further investigation is warranted.

The results obtained with the modified inlets indicate that the design of these internal-contraction inlets should include three factors. These factors are: (a) a gradual fairing of the entrance to the subsonic diffuser, (b) an internal shape which is as nearly axially symmetric as is consistent with the method of shape variation, and (c) a uniform rate of pressure rise during supersonic compression.

Ames Aeronautical Laboratory
National Advisory Committee for Aeronautics
Moffett Field, Calif., June 23, 1955

REFERENCES

1. Watson, Earl C.: An Analytical Study of the Comparative Performance of Six Air-Induction Systems for Turbojet-Powered Airplanes Designed to Operate at Mach Numbers up to 2.0. NACA RM A53H03, 1953.
2. Gorton, Gerald C.: Investigation of Translating-Spike Supersonic Inlet as a Means of Mass-Flow Control at Mach Numbers of 1.5, 1.8, and 2.0. NACA RM E53G10, 1953.
3. Gorton, Gerald C.: Investigation at Supersonic Speeds of a Translating-Spike Inlet Employing a Steep-Lip Cowl. NACA RM E54G29, 1954.
4. Gorton, Gerald C., and Dryer, Murry: Comparison at Supersonic Speeds of Translating-Spike Inlets Having Blunt- and Sharp-Lip Cowls. NACA RM E54J07, 1955.
5. Scherrer, Richard, Stroud, John F., and Swift, John T.: Preliminary Investigation of a Variable-Area Auxiliary Air-Intake System at Mach Numbers From 0 to 1.3. NACA RM A53A13, 1953.
6. Allen, J. L., and Beke, Andrew: Force and Pressure Recovery Characteristics at Supersonic Speeds of a Conical Spike Inlet With a Bypass Discharging from the Top or Bottom of the Diffuser in an Axial Direction. NACA RM E53A29, 1953.
7. Leissler, L. Abbott, and Nettles, J. Cary: Investigation to a Mach Number of 2.0 of Shock-Positioning Controls for Variable Geometry Inlet in Combination With a J-34 Turbojet. NACA RM E54I27, 1954.
8. Schueller, Carl F., and Esenwein, Fred T.: Analytical and Experimental Investigation of Inlet-Engine Matching for Turbojet-Powered Aircraft at Mach Numbers up to 2.0. NACA RM E51K20, 1952.

9. Comenzo, Raymond J.: A Preliminary Investigation of the Pressure Recovery of Several Two-Dimensional Supersonic Inlets at a Mach Number of 2.01. NACA RM L54D14, 1954.
10. Stitt, Leonard J., and Wise, George A.: Investigation of Several Double-Ramp Side Inlets. NACA RM E54D20, 1954.
11. Davis, Wallace F., Brajnikoff, George B., Goldstein, David L., and Spiegel, Joseph M.: An Experimental Investigation at Supersonic Speeds of Annular Duct Inlets Situated in a Region of Appreciable Boundary Layer. NACA RM A7G15, 1947.
12. Lukasiewicz, J.: Supersonic Diffusers ARC. R. & M. No. 2501, British R.A.E., June 1946.
13. Staff of Ames Aeronautical Laboratory: Equations, Tables, and Charts for Compressible Flow. NACA Rep. 1135, 1953.
14. Oswatitsch, K. I.: Pressure Recovery for Missiles With Reaction Propulsion at High Supersonic Speeds (The Efficiency of Shock Diffusers). NACA TM 1140, 1947.

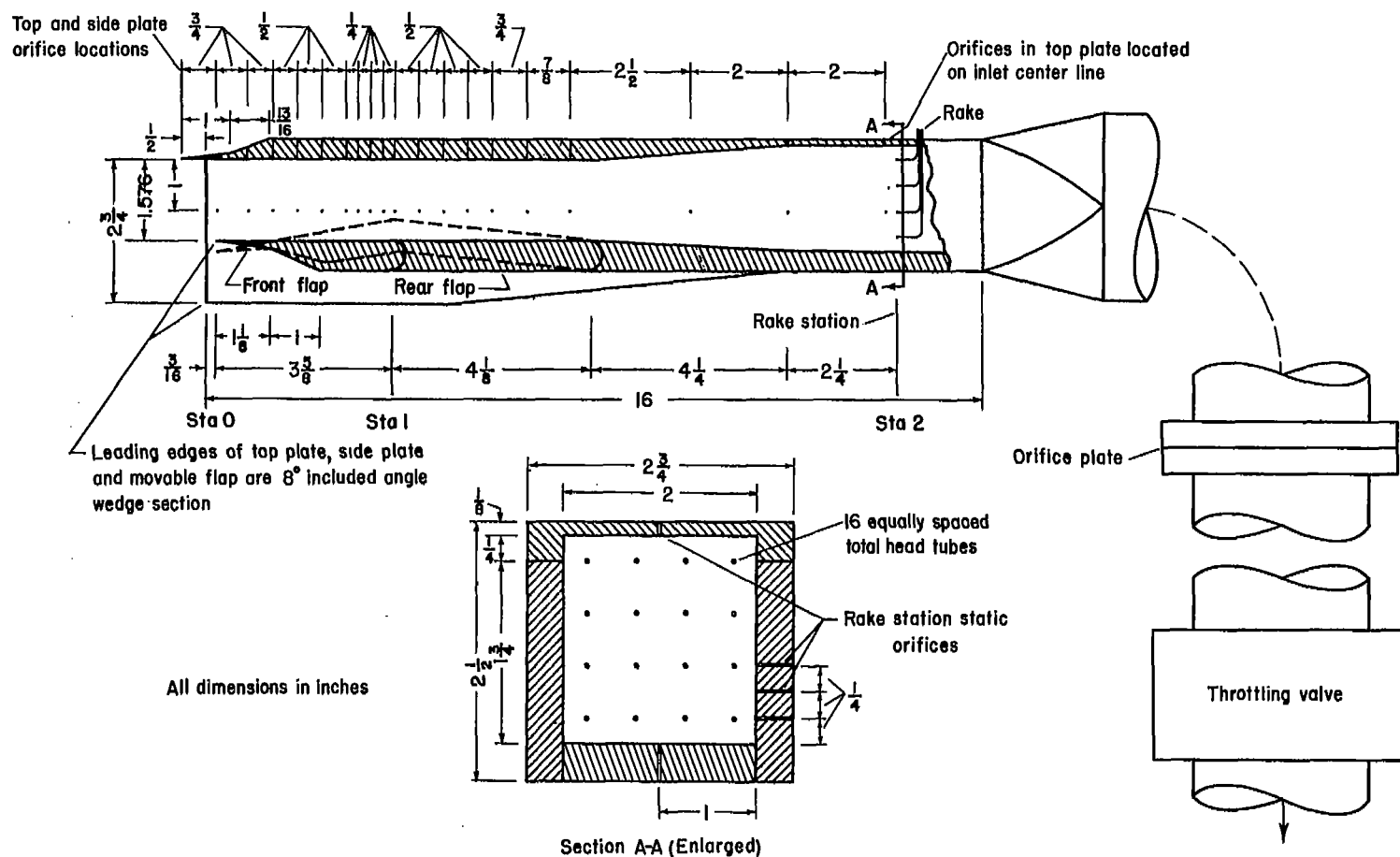


Figure 1.- Sketch showing general arrangement and instrumentation for variable-area, variable-internal-contraction inlet.

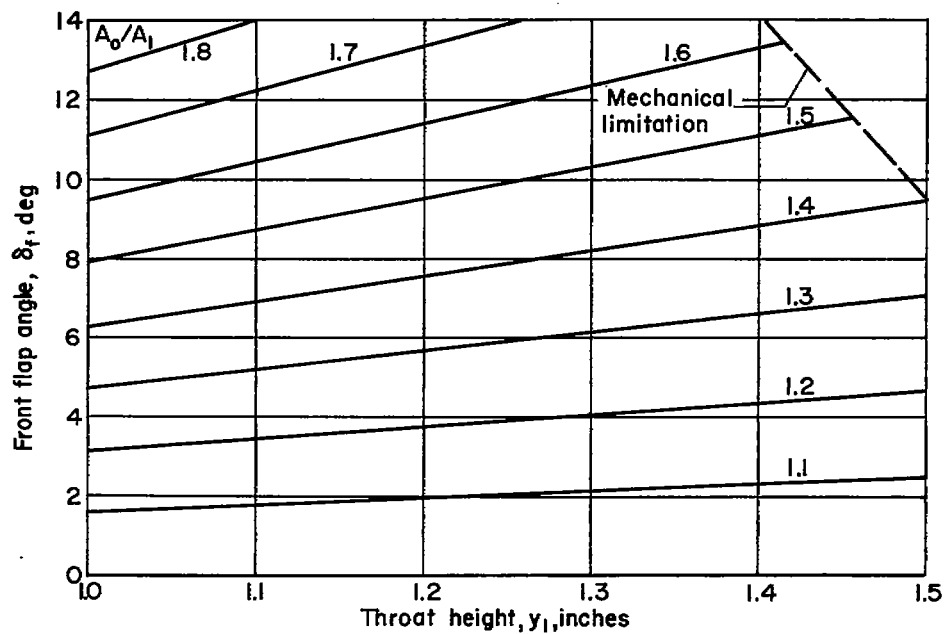
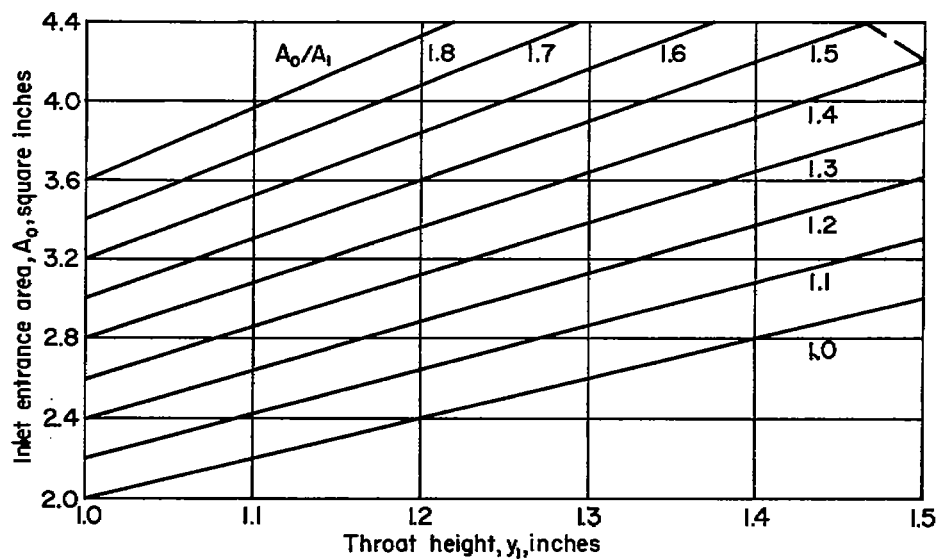
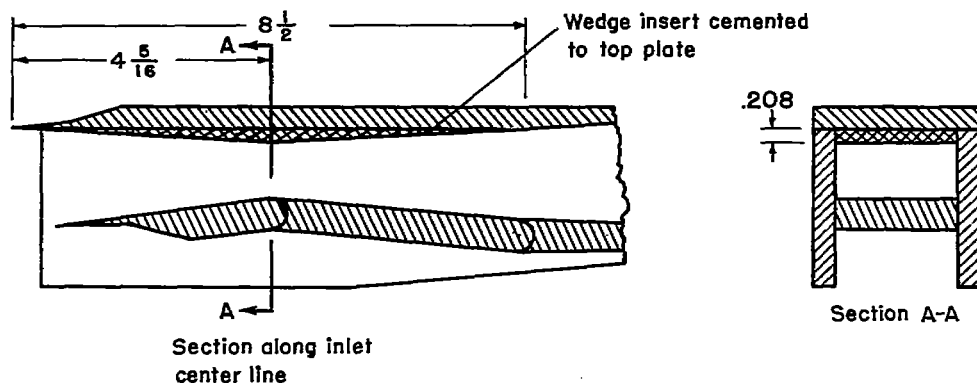
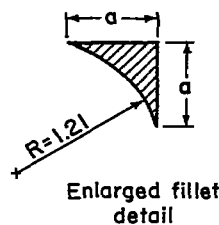
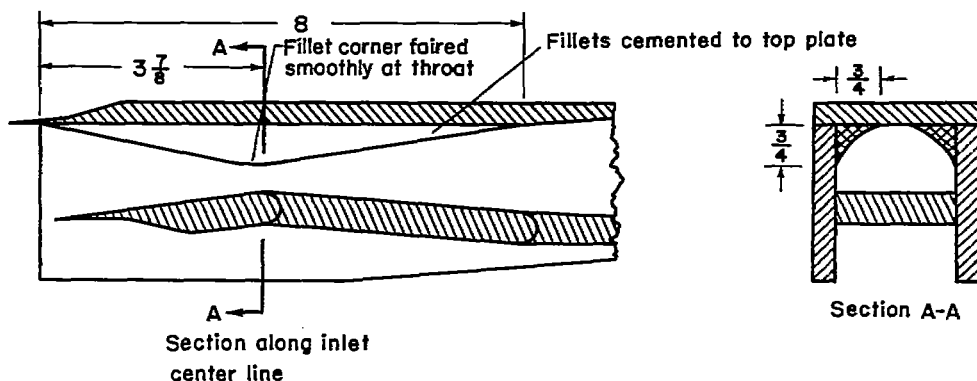
(a) Front flap angle, δ_f .(b) Inlet entrance area, A_0 .

Figure 2.- Variation of several geometric parameters with inlet throat height for various contraction ratios.



Wedge insert installation

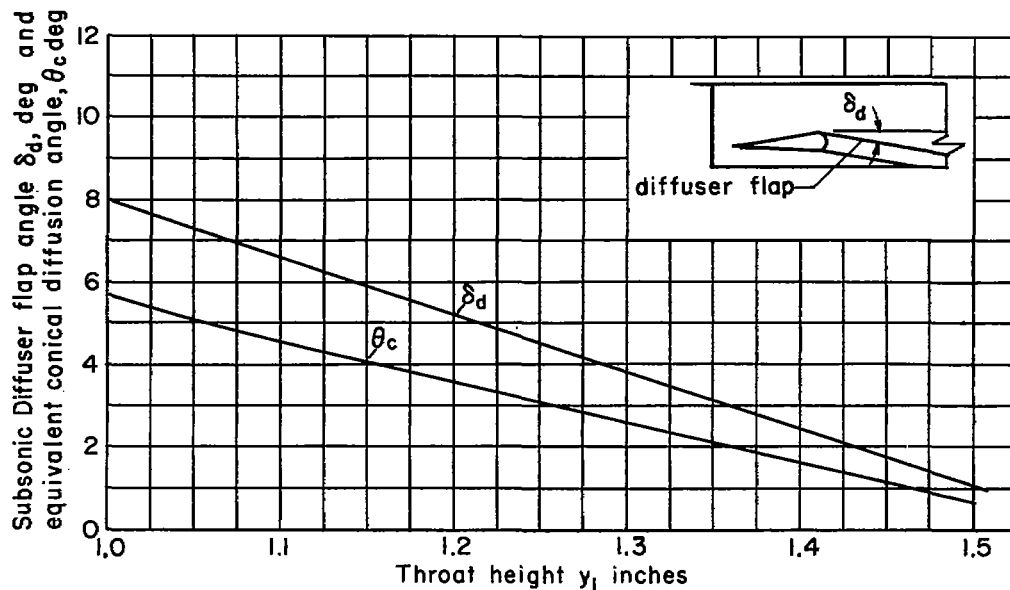


All sections of fillet were similar with some fillet radius but with dimension a varying from 0 to 0.75 inch.

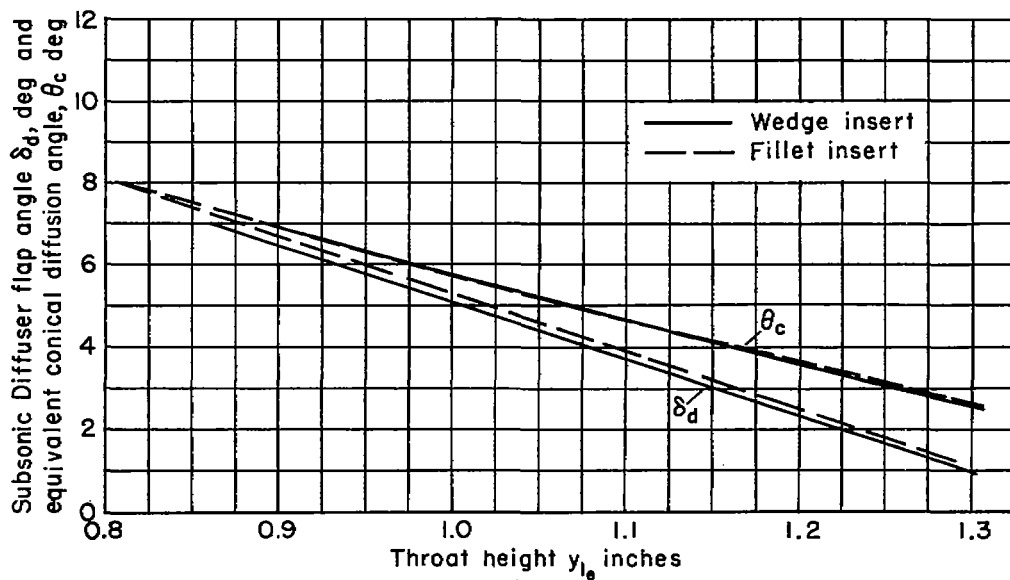
Fillet insert installation

- Note 1. All dimensions in inches
2. Wedge and fillet installations provided about the same contraction ratio at the throat

Figure 3.- Sketches showing the details of the wedge and fillet installation.



(a) Original inlet.



(b) Inlet with wedge or fillet inserts.

Figure 4.- Variation of subsonic diffuser flap angle and equivalent conical diffusion angle with throat height.

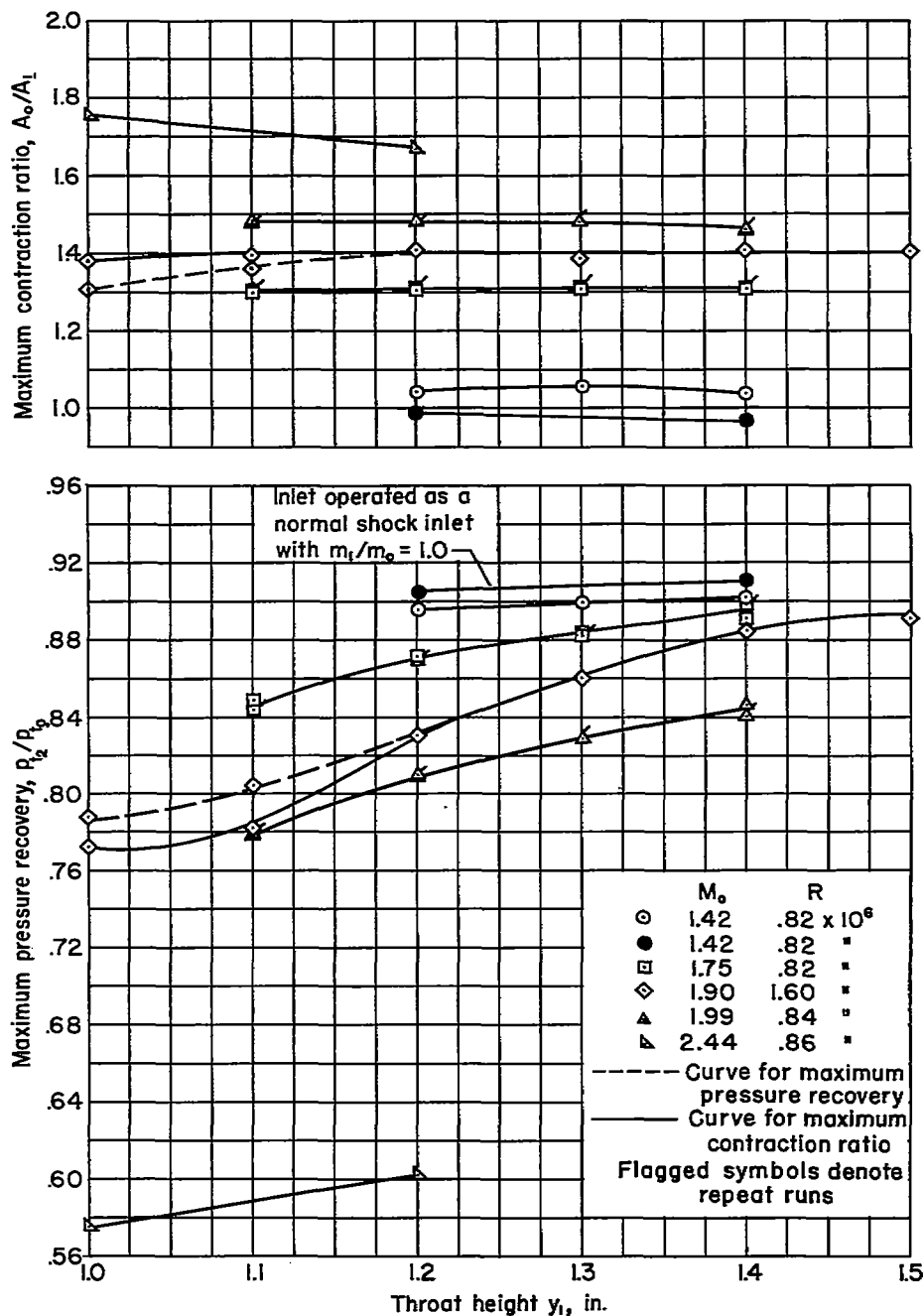
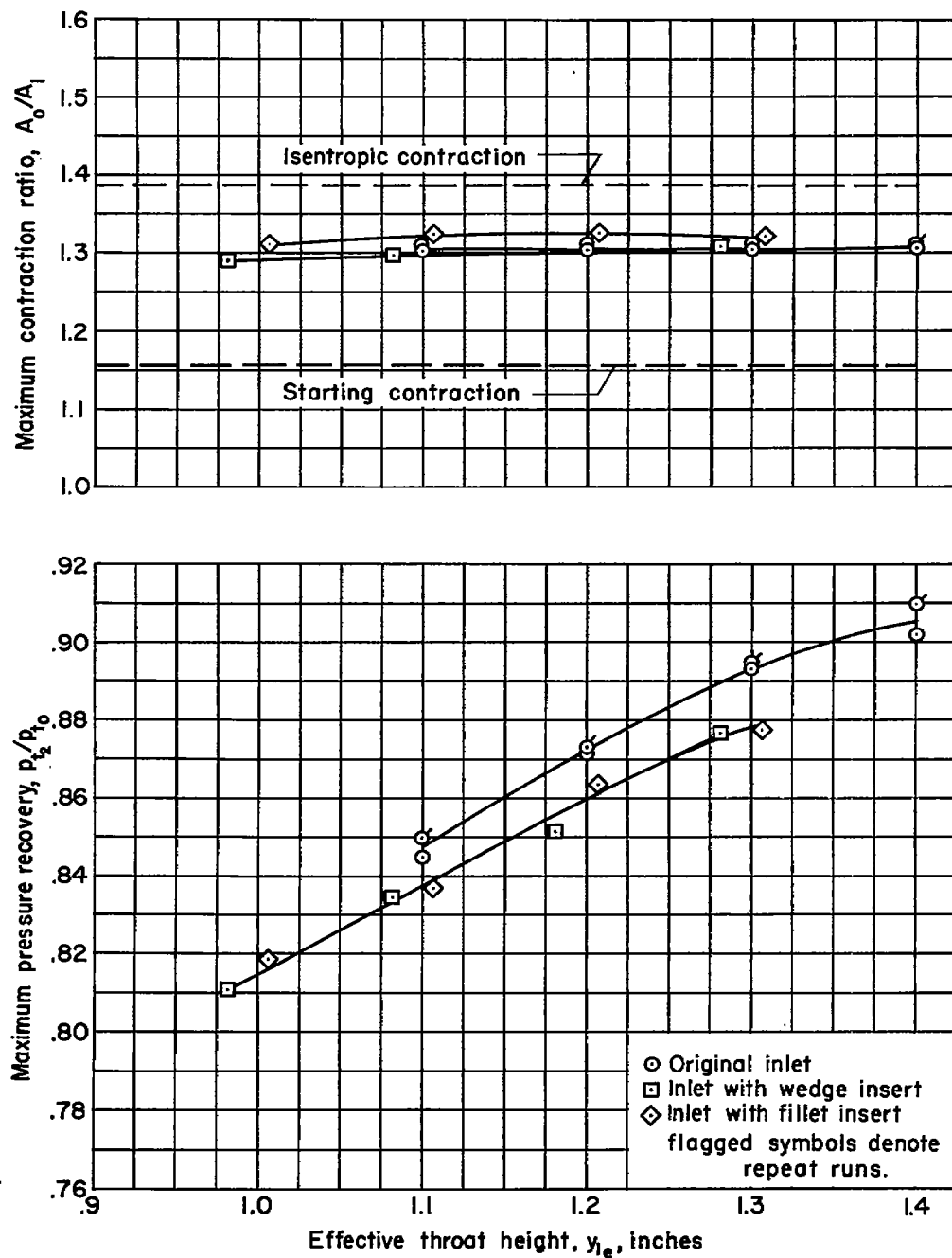
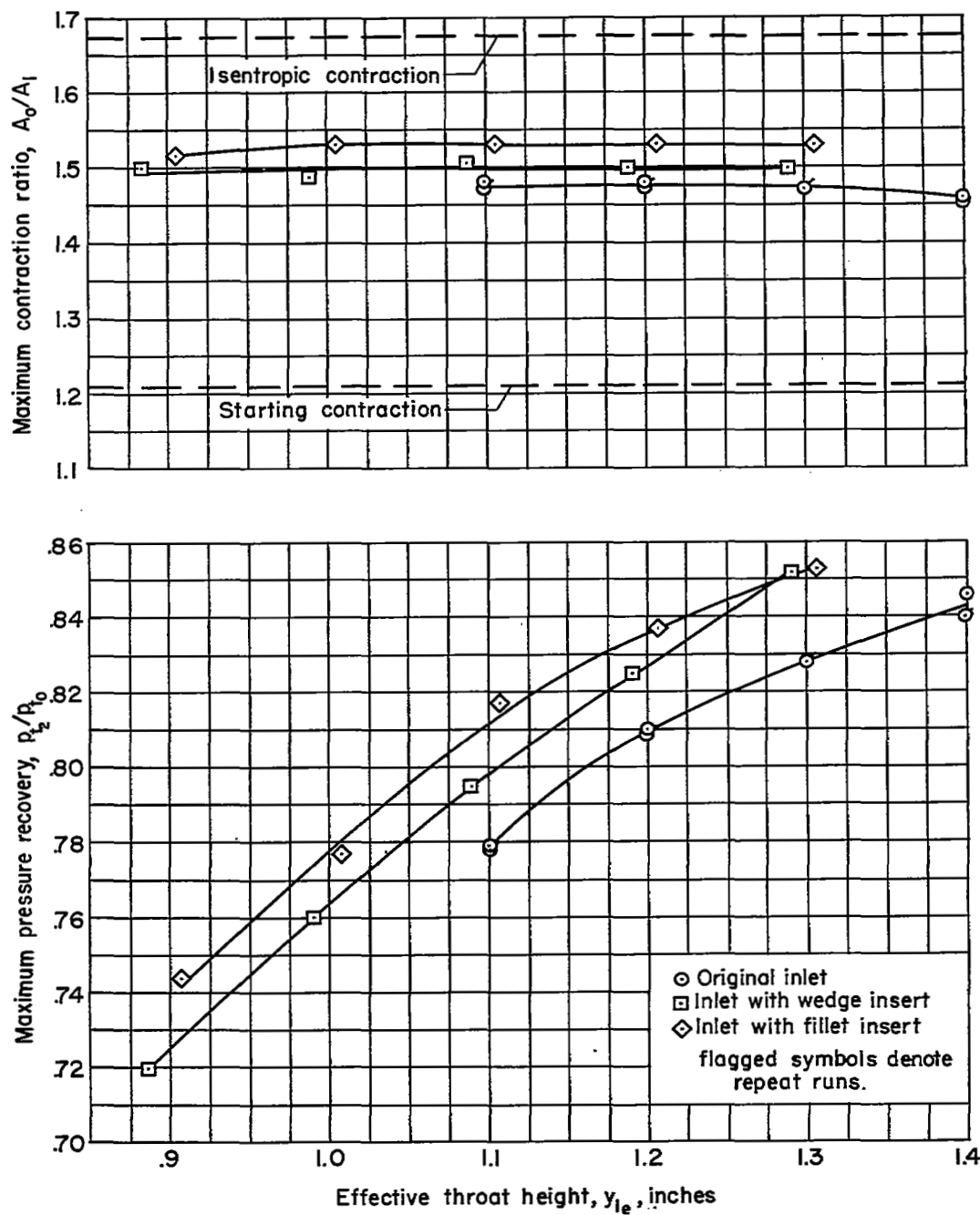


Figure 5.- Variation of maximum pressure recovery and maximum contraction ratio with inlet throat height for the unmodified inlet at Mach numbers from 1.42 to 2.44.



(a) $M_0 = 1.75$; $R = 0.84 \times 10^6$

Figure 6.- Comparison of the peak performance of the inlets with modified and unmodified internal geometry.



(b) $M_o = 1.99$; $R = 0.84 \times 10^6$

Figure 6.- Concluded.

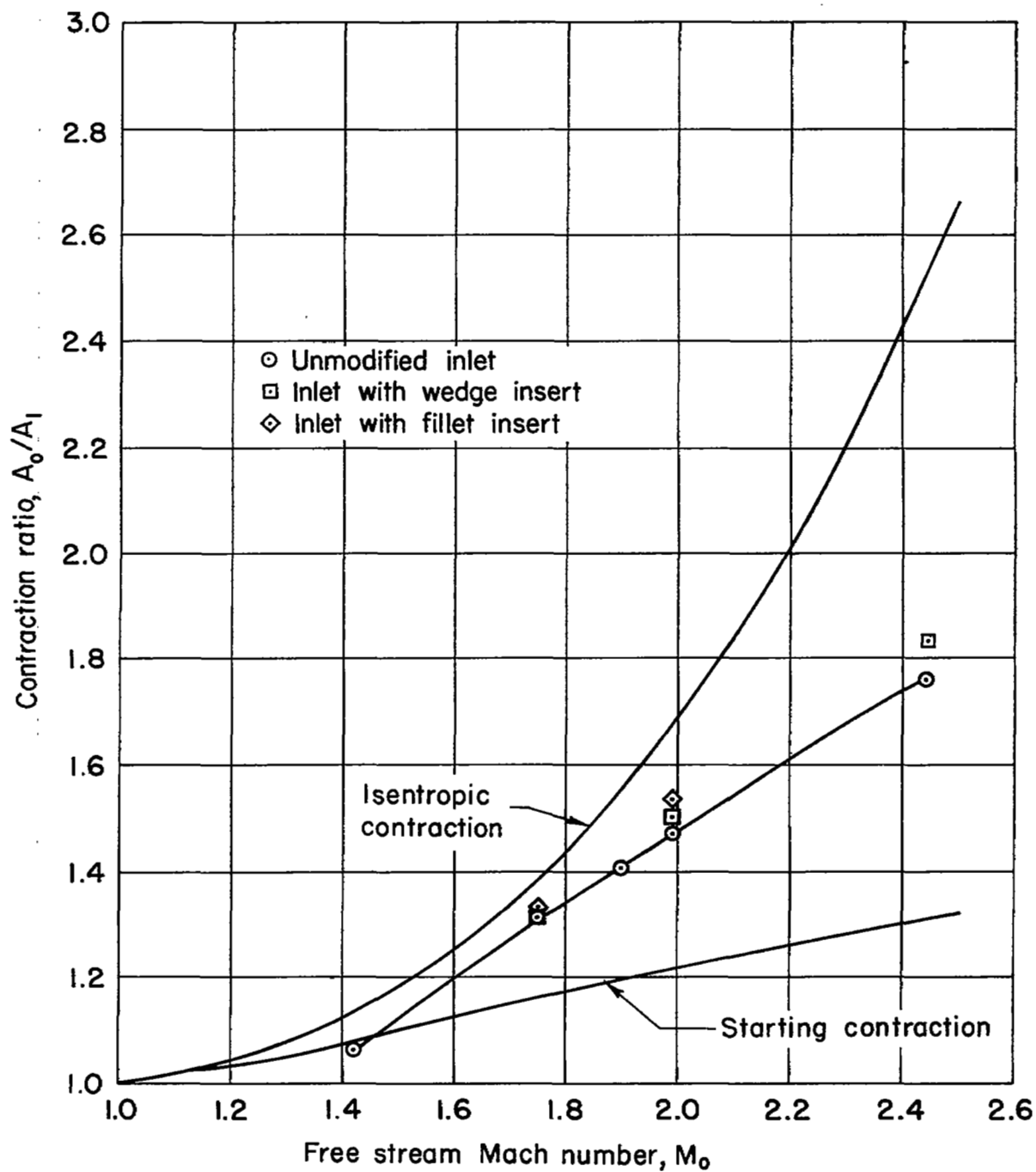
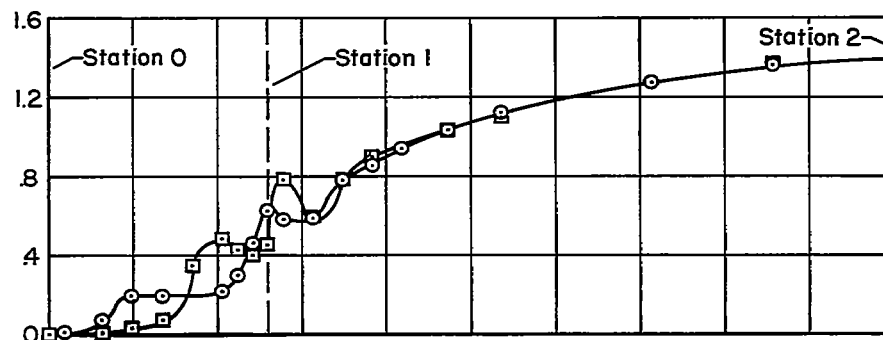
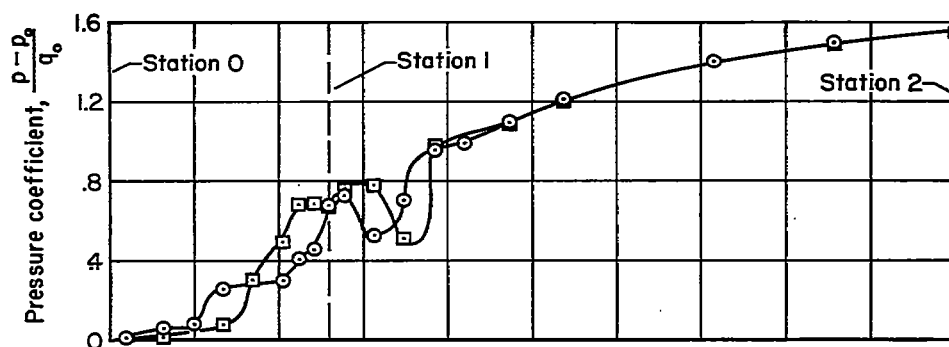
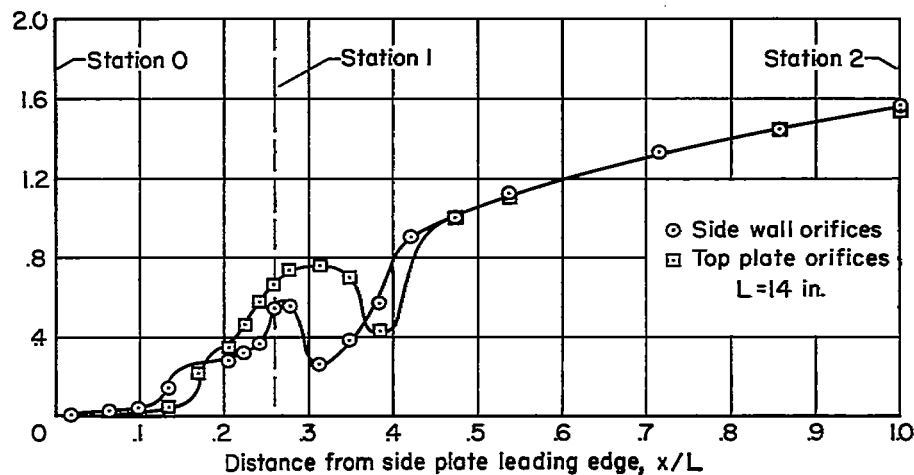


Figure 7.- Variation of maximum contraction ratio with free-stream Mach number.

(a) $M_o = 1.75$; $y_1 = 1.300$; $A_o/A_1 = 1.303$ (b) $M_o = 1.99$; $y_1 = 1.30$; $A_o/A_1 = 1.455$ (c) $M_o = 2.44$; $y_1 = 1.200$; $A_o/A_1 = 1.668$ Figure 8.- Typical longitudinal static-pressure distributions for the unmodified inlet at three Mach numbers ($R = 0.84 \times 10^6$).

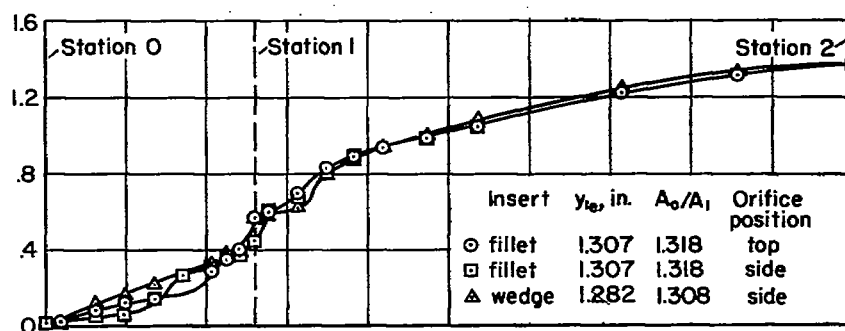
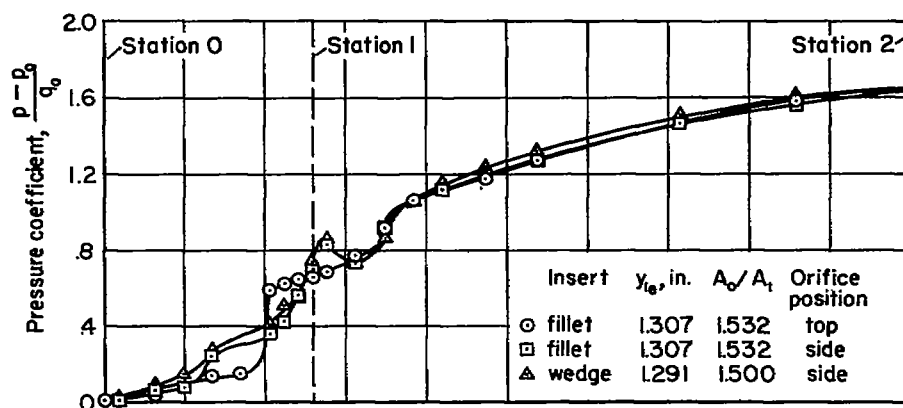
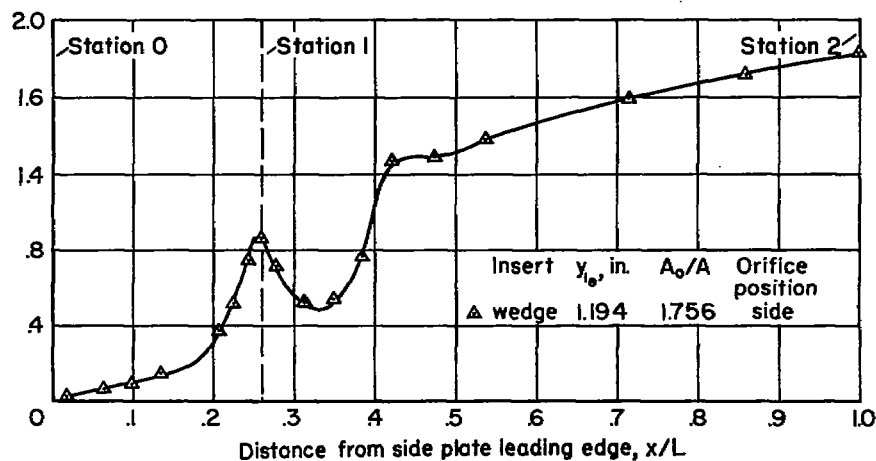
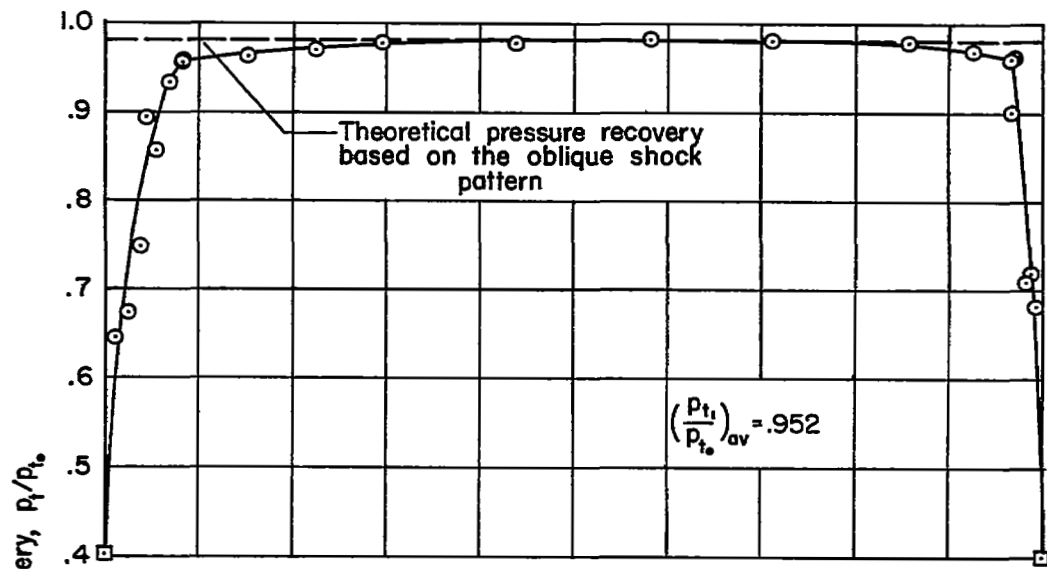
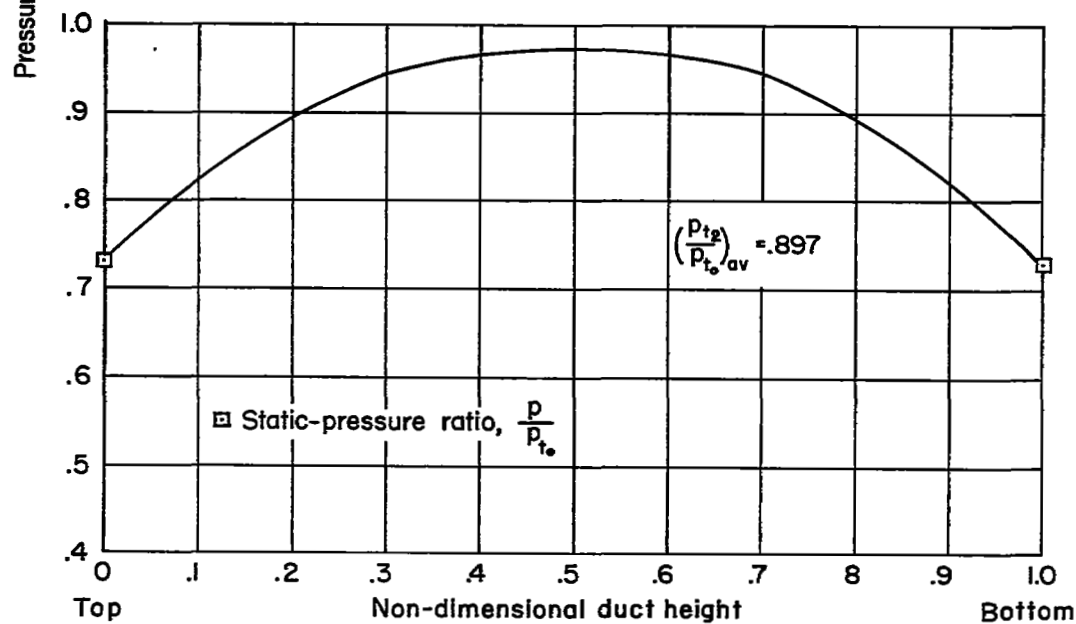
(a) $M_O = 1.75$ (b) $M_O = 1.99$ (c) $M_O = 2.44$

Figure 9.- Typical longitudinal static-pressure distributions for the inlet with wedge- and fillet-type inserts at three Mach numbers ($R = 0.84 \times 10^6$).



(a) Pitot survey near throat.



(b) Distribution at rake station.

Figure 10.- Comparison of the vertical center-line distributions of pressure recovery at the throat and rake stations for the unmodified inlet ($y_1 = 1.40$ inches; $A_0/A_1 = 1.410$; $M = 1.90$; $R = 1.60 \times 10^6$).

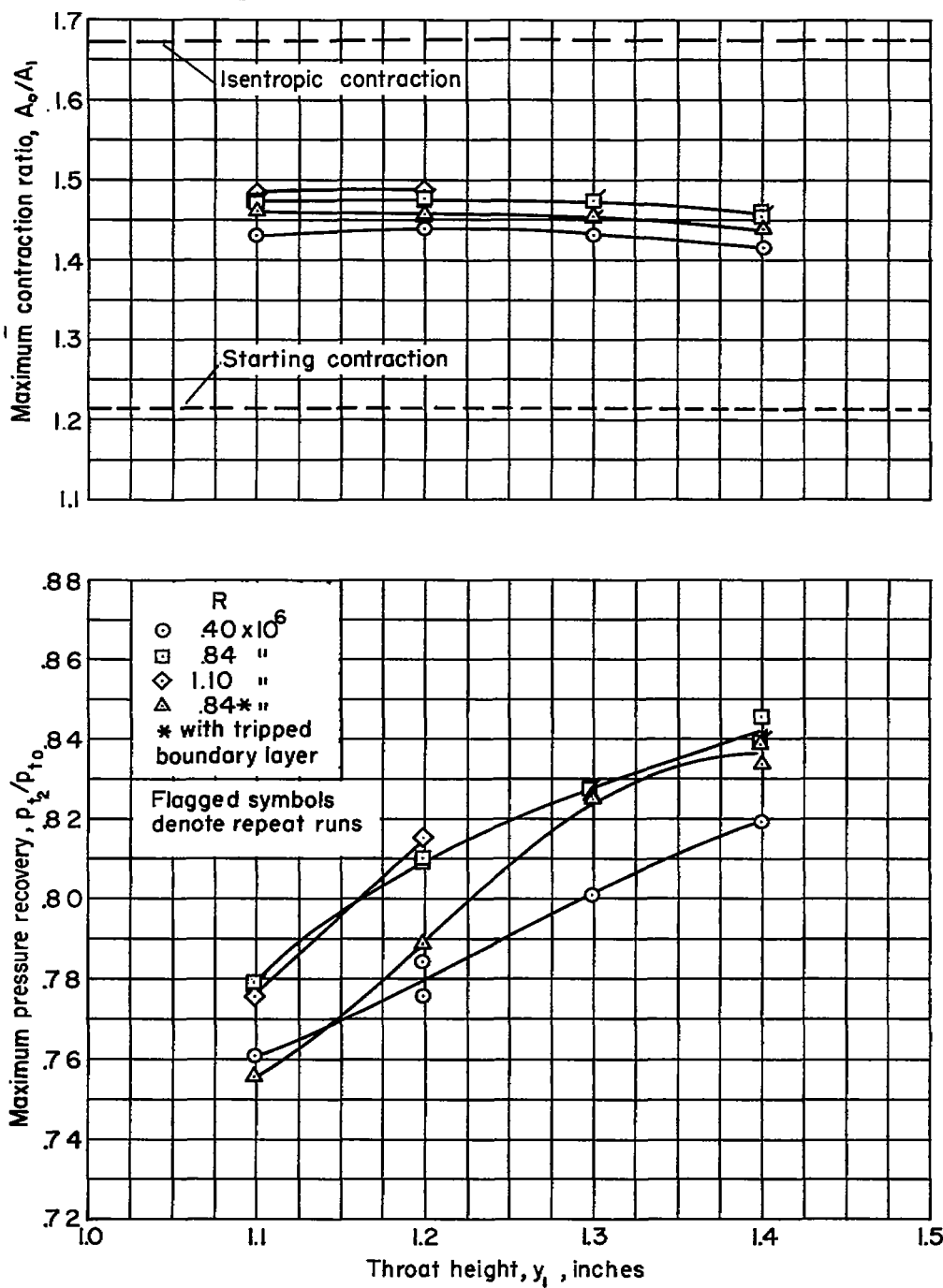
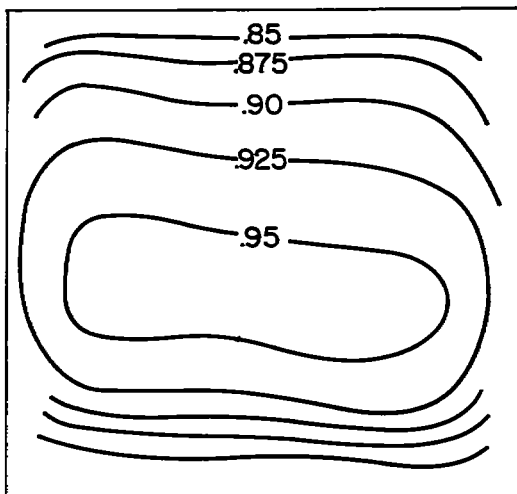
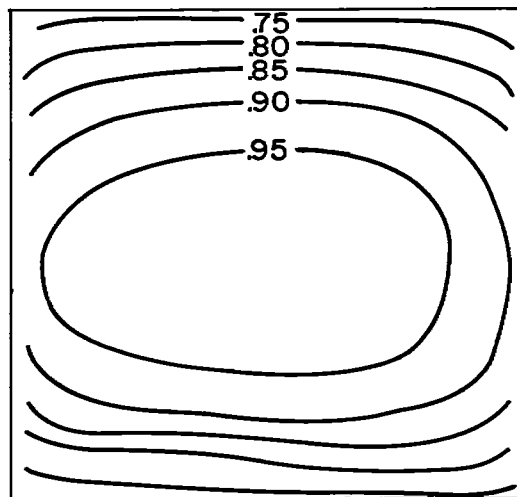


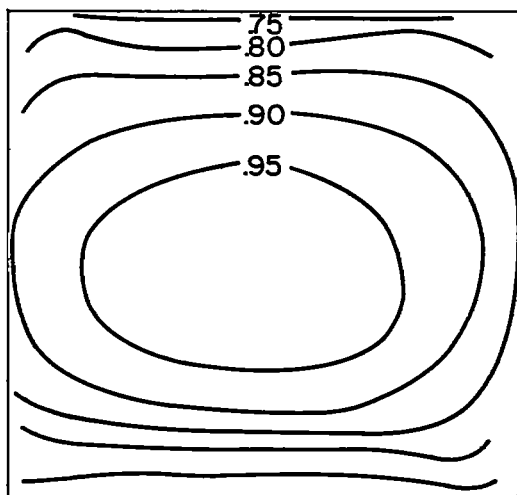
Figure 11.- Effect of variation of Reynolds number on inlet performance for the unmodified inlet at a Mach number of 1.99.



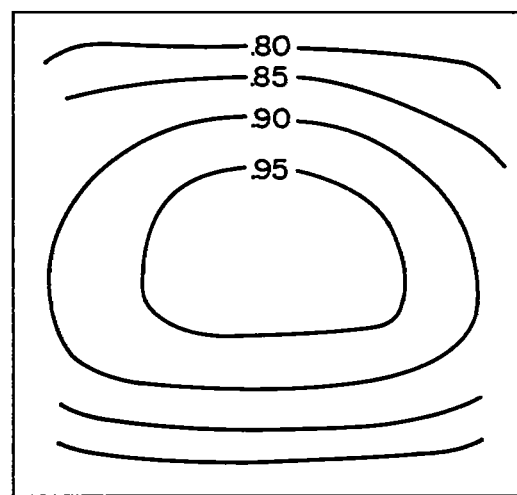
(a) $M_O = 1.42$; $R = 0.82 \times 10^6$;
 $y_1 = 1.40$; $A_O/A_1 = 0.968$
 (Operating as a normal-shock inlet)



(b) $M_O = 1.42$; $R = 0.82 \times 10^6$;
 $y_1 = 1.40$; $A_O/A_1 = 1.033$

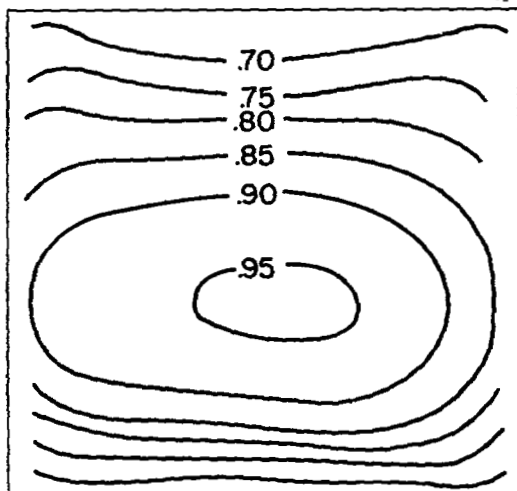


(c) $M_O = 1.75$; $R = 0.82 \times 10^6$;
 $y_1 = 1.40$; $A_O/A_1 = 1.304$

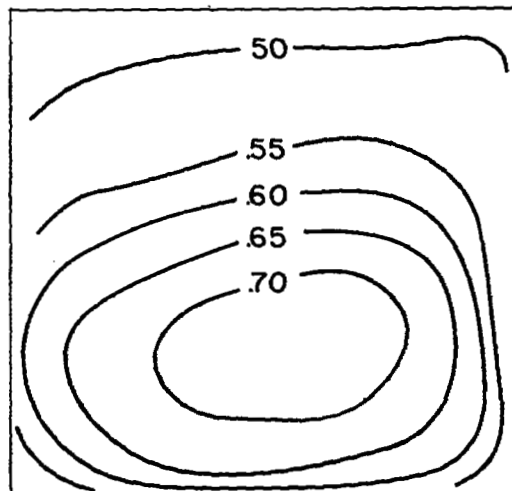


(d) $M_O = 1.90$; $R = 1.60 \times 10^6$;
 $y_1 = 1.40$; $A_O/A_1 = 1.400$

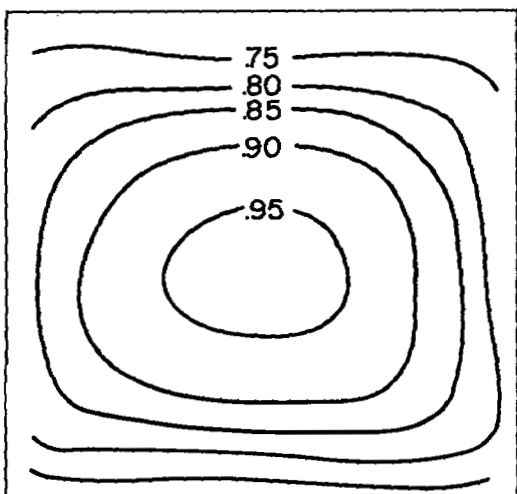
Figure 12.- Typical distributions of pressure recovery at the rake station for each Mach number.



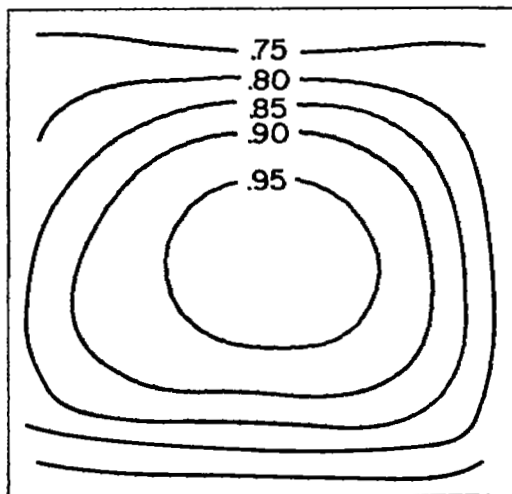
(e) $M_0 = 1.99$; $R = 0.84 \times 10^6$;
 $y_1 = 1.40$; $A_0/A_1 = 1.455$



(f) $M_0 = 2.44$; $R = 0.86 \times 10^6$;
 $y_1 = 1.20$; $A_0/A_1 = 1.669$



(g) $M_0 = 1.99$; $R = 0.84 \times 10^6$;
 $y_1 = 1.291$; $A_0/A_1 = 1.500$;
 model with wedge insert.



(h) $M_0 = 1.99$; $R = 0.84 \times 10^6$;
 $y_{1e} = 1.307$; $A_0/A_1 = 1.532$;
 model with fillet insert.

Figure 12.- Concluded.

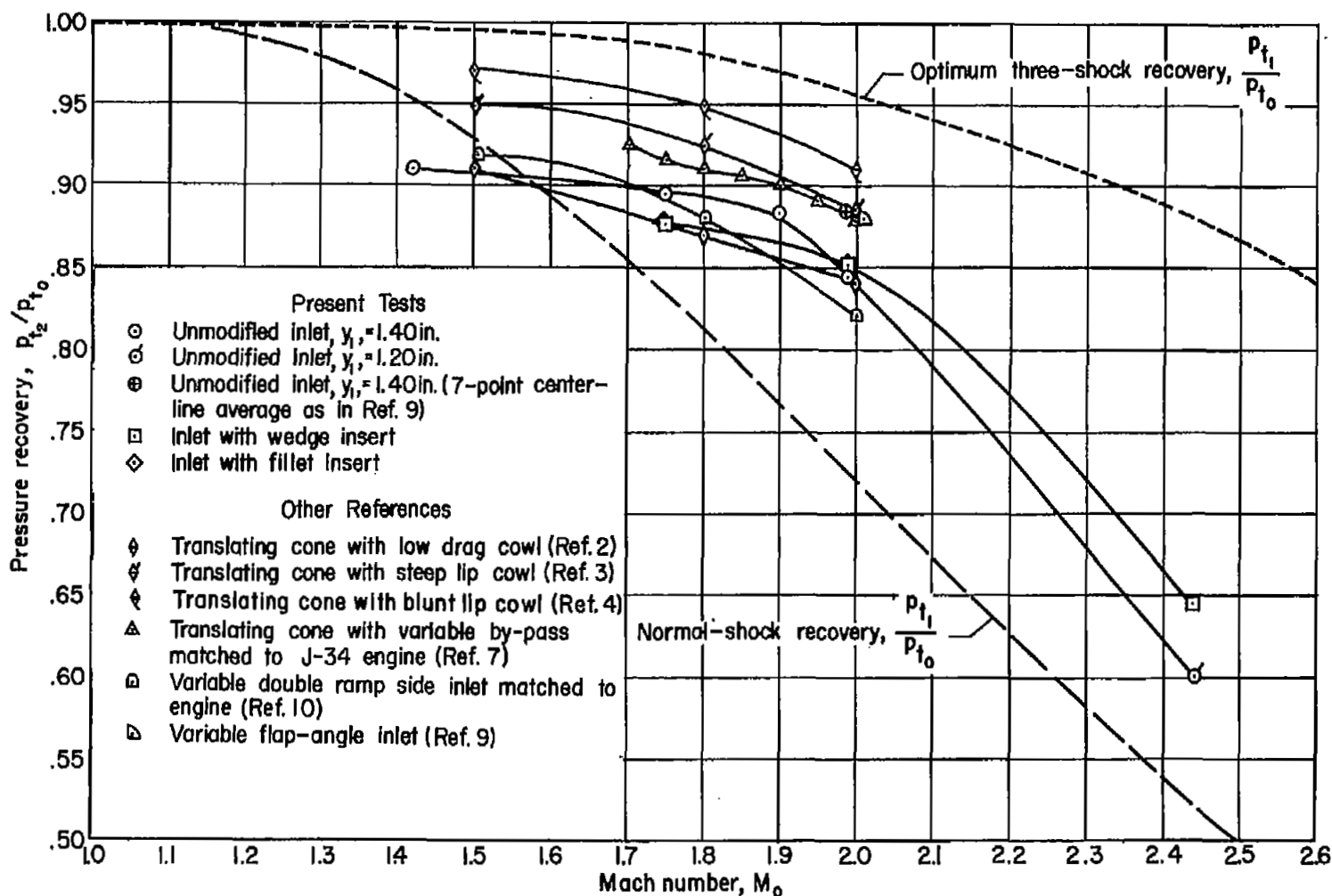


Figure 13.- Comparison of the maximum pressure-recovery characteristics of the variable-area, variable-internal-contraction inlet with the pressure recovery obtained with other inlets.



3 1176 01434 8636

